Solutions of the Quasi-Vector Wave Equation for Optical Waveguides in a Mapped Infinite Domains by the Galerkin's Method

Kai Ming Lo and E. Herbert Li, *Senior Member, IEEE*

Abstract— **Galerkin's method is employed to analyze the quasi-vector wave equation for optical waveguides with arbitrary refractive index profile in a mapped infinite domains. Results are presented for a range of waveguide structures which include rectangular core, circular core, rib, and multiple quantum well. Solutions are compared favorably with exact vector solution and numerical results using Fourier operator transform method and beam propagation method.**

I. INTRODUCTION

THE use of Galerkin's method in solving the scalar wave equation of optical waveguides with arbitrary refractive index profiles was first proposed by Henry and Verbeek [1]. Same method was used by Marcuse in solving the vector wave equation [2]. However, there is a large increase in computing time and memory. In considering that matter, we decide to use the quasi-vector results which include the polarization effects of optical waveguides as an intermediate solution. The memory requirement is the same as in solving the scalar wave equation while the computing time is moderate.

We also employ a mapping scheme to eliminate the need of enclosing waveguide structures within a rectangle whose size affect the accuracy of calculations near modal cutoff [3]. Alternately, the elimination can be done by using Hermite-Gauss functions as basis functions [4] rather than sine functions which are used in present studies. However, such elimination is only valid for waveguides with homogeneous cladding. For inhomogeneous cladding waveguides like rib waveguides, the cladding have to be truncated if Hermite-Gauss basis functions are used. On the other hand, no truncation of cladding is needed if sine basis functions are used in a mapped infinite domains.

In the next section, we will derive the quasi-vector wave equation and establish the details of solving this equation using the Galerkin's method. In Section III, we compare some of our numerical results with those of other authors. The summary section anticipates the range of potential applications of present method.

II. MATHEMATICAL FORMULATION

A. Quasi-vector wave equation

Maxwell's equations are employed to calculate the spatial variation of electric field $\mathbf{E}(x, y, z)$ and magnetic field $\mathbf{H}(x, y, z)$ of an optical waveguide. The dielectric constant $\varepsilon(x, y, z)$ of a waveguide is related to its refractive index $n(x, y, z)$ by $\varepsilon = n^2 \varepsilon_0$, where ε_0 is the free space electric permittivity. The magnetic permeability is taken to have its free

The authors are with the Department of Electrical and Electronic Engineering, The University of Hong Kong, Pokfulam Road, Hong Kong.
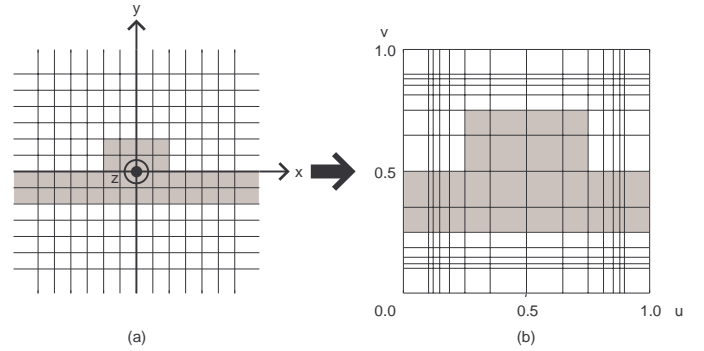

Fig. 1. An optical structure in (a) x-y plane and (b) transformed u-v domains. A rib waveguide is used as an example.

space value ($\mu = \mu_0$) everywhere. The field vectors are taken to depend on time through the implicit factor $\exp(-i\omega t)$. Under these conditions and regions are free of charges and current, Maxwell's equations are written as

$$\boldsymbol{\nabla} \times \mathbf{E} = i(\mu_0/\varepsilon_0)^{1/2} k \mathbf{H} , \qquad (1)$$

$$\boldsymbol{\nabla} \times \mathbf{H} = -i(\varepsilon_0/\mu_0)^{1/2} k n^2 \mathbf{E} , \qquad (2)$$

where $k = 2\pi/\lambda$ is the free space wavenumber, and λ is the wavelength of light in free space.

If we eliminate the magnetic field from (1) and (2) by $\boldsymbol{\nabla} \times (1)$ and substitute $\boldsymbol{\nabla} \times \mathbf{H}$ from (2) into, we obtain the vector wave equation

$$(\boldsymbol{\nabla}^2 + k^2 n^2)\mathbf{E} = -\boldsymbol{\nabla}(\mathbf{E} \cdot \boldsymbol{\nabla} \ln n^2) \qquad (3)$$

by using two vector identities, viz.

$$\boldsymbol{\nabla} \times (\boldsymbol{\nabla} \times \mathbf{E}) = \boldsymbol{\nabla}(\boldsymbol{\nabla} \cdot \mathbf{E}) - \boldsymbol{\nabla}^2 \mathbf{E} , \qquad (4)$$

$$\boldsymbol{\nabla} \cdot (n^2 \mathbf{E}) = n^2 \boldsymbol{\nabla} \cdot \mathbf{E} + \mathbf{E} \cdot \boldsymbol{\nabla} n^2 = 0 . \qquad (5)$$

The $\boldsymbol{\nabla}^2$ in (3) is a vector operator. However, if the field vectors have components referred to fixed cartesian directions x, y and z as indicated in Fig. 1(a), the vector operator $\boldsymbol{\nabla}^2$ is replaced by the scalar Laplacian ∇^2. Moreover, if an optical waveguide with refractive index profile that does not change with distance z along the waveguide, i.e. $n = n(x, y)$. The electric field of the waveguide can be written in separable form as

$$\mathbf{E}(x, y, z) = \mathbf{e}(x, y) \exp(i\beta z) \qquad (6)$$

where β is the propagation constant. Thus if we set

$$\mathbf{e} = e_x \hat{\mathbf{x}} + e_y \hat{\mathbf{y}} + e_z \hat{\mathbf{z}} \qquad (7)$$

in (6) where $\hat{\mathbf{x}}$, $\hat{\mathbf{y}}$ and $\hat{\mathbf{z}}$ are unit vector parallel to the axes in Fig. 1(a) and using

$$\boldsymbol{\nabla}^2 = \nabla^2 = \frac{\partial^2}{\partial x^2} + \frac{\partial^2}{\partial y^2} - \beta^2 , \tag{8}$$

(3) is reduced to two equations coupling the field components e_x and e_y as follows:

$$\frac{\partial^2 e_x}{\partial x^2} + \frac{\partial^2 e_x}{\partial y^2} + (k^2 n^2 - \beta^2)e_x$$
$$+ 2\frac{\partial}{\partial x}\left(e_x\frac{\partial \ln n}{\partial x} + e_y\frac{\partial \ln n}{\partial y}\right) = 0 , \tag{9}$$

$$\frac{\partial^2 e_y}{\partial x^2} + \frac{\partial^2 e_y}{\partial y^2} + (k^2 n^2 - \beta^2)e_y$$
$$+ 2\frac{\partial}{\partial y}\left(e_x\frac{\partial \ln n}{\partial x} + e_y\frac{\partial \ln n}{\partial y}\right) = 0 . \tag{10}$$

If the coupling terms in (9) and (10) are neglected, we have

$$\frac{\partial^2 e_x}{\partial x^2} + \frac{\partial^2 e_x}{\partial y^2} + (k^2 n^2 - \beta^2)e_x$$
$$+ 2\frac{\partial}{\partial x}\left(e_x\frac{\partial \ln n}{\partial x}\right) = 0 , \tag{11}$$

$$\frac{\partial^2 e_y}{\partial x^2} + \frac{\partial^2 e_y}{\partial y^2} + (k^2 n^2 - \beta^2)e_y$$
$$+ 2\frac{\partial}{\partial y}\left(e_y\frac{\partial \ln n}{\partial y}\right) = 0 . \tag{12}$$

These are in fact the scalar wave equation with polarization correction which are referred here as the quasi-TE wave equation and the quasi-TM wave equation.

The assumption used in (11) and (12), i.e. $e_x \gg e_y$ in (11) and $e_y \gg e_y$ in (12), is accurate for three classes of waveguides [5]: (i) weakly guiding waveguides [6] with arbitrary shape and small difference in refractive index between core and cladding or substrate, (ii) rectangular core waveguides with arbitrary core-cladding refractive index operated in the far-from-cutoff region, (iii) arbitrary refractive index profile waveguides with an elongated or slab like cross section. Numerical results for these three classes of waveguides will be given in Section III.

B. Galerkin's method

Since the formulation of the quasi-vector wave equation (11) and (12) are the same, the quasi-TE wave equation (11) will be solved below using Galerkin's method and the procedure developed is applicable for solving the quasi-TM wave equation (12).

To eliminate the need of enclosing waveguide within a rectangle, the whole x-y plane is mapped onto a unit square in u-v space as shown in Fig. 1 using the transformation functions:

$$x = \alpha_x \tan\left[\pi\left(u - \frac{1}{2}\right)\right] , \tag{13}$$

$$y = \alpha_y \tan\left[\pi\left(v - \frac{1}{2}\right)\right] , \tag{14}$$

where α_x and α_y are scaling parameters in the x and y directions respectively. The same change of variables is applied to the quasi-TE wave equation (11) and in the u-v space it is written as

$$\left(\frac{du}{dx}\right)^2 \frac{\partial^2 e_x}{\partial u^2} + \frac{d^2u}{dx^2}\frac{\partial e_x}{\partial u} + \left(\frac{dv}{dy}\right)^2 \frac{\partial^2 e_x}{\partial v^2} + \frac{d^2v}{dy^2}\frac{\partial e_x}{\partial v}$$
$$+ (n^2k^2 - \beta^2)e_x + 2\left(\frac{du}{dx}\right)^2 \frac{\partial}{\partial u}\left(e_x\frac{\partial \ln n}{\partial u}\right)$$
$$+ 2\frac{d^2u}{dx^2}e_x\frac{\partial \ln n}{\partial u} = 0 \tag{15}$$

where $e_x = e_x(u,v)$, $n = n(u,v)$.

The unknown electric field component e_x is expanded as

$$e_x = \sum_i^{N_m N_n} a_i \phi_i(u,v) = \sum_{m_i=1}^{N_m}\sum_{n_i=1}^{N_n} a_{m_i,n_i}\phi_i(u,v) \tag{16}$$

where integer quotient function div and remainder on division function mod are employed to relate the index, i, and spatial frequencies, m_i and n_i, as

$$m_i = (i-1)\,\mathrm{div}\,N_n + 1 , \tag{17}$$
$$n_i = (i-1)\,\mathrm{mod}\,N_n + 1 . \tag{18}$$

The expansion functions $\phi_i(u,v)$ are chosen as the complete set of orthonormal sine basis functions as

$$\phi_i(u,v) = 2\sin(m_i\pi u)\sin(n_i\pi v) . \tag{19}$$

The field expansion (16) is substituted into (15), it is then multiplied by $\phi_j(u,v)$ and integrated over the unit square in Fig. 1(b) and yield the result:

$$\sum_i^{N_m N_n} (S_{j,i} + P_{j,i} - W^2\delta_{j,i})a_i = 0 \tag{20}$$

where

$$S_{j,i} = V^2 A_{j,i} + B_{j,i} \tag{21}$$

correspond to the scalar wave equation with

$$A_{j,i} = \int_{u=0}^1 \int_{v=0}^1 g(u,v)\phi_i(u,v)\phi_j(u,v)dudv , \tag{22}$$
$$B_{j,i} = \rho^2(I_1 + I_2 + I_3 + I_4) , \tag{23}$$

and

$$g(u,v) = \frac{n^2(u,v) - n_{\mathrm{cl}}^2}{n_{\mathrm{co}}^2 - n_{\mathrm{cl}}^2} . \tag{24}$$

Here, $\delta_{j,i}$ is a delta function and defined as

$$\delta_{j,i} = \begin{cases} 1 & \text{if } j = i , \\ 0 & \text{if } j \neq i . \end{cases} \tag{25}$$

The modal parameters V and W are defined as

$$V = k\rho(n_{\mathrm{co}}^2 - n_{\mathrm{cl}}^2)^{1/2} , \tag{26}$$
$$W = \rho(\beta^2 - k^2 n_{\mathrm{cl}}^2)^{1/2} . \tag{27}$$

The core and cladding refractive index, n_{co} and n_{cl}, and normalization parameter ρ are chosen to be representative of the
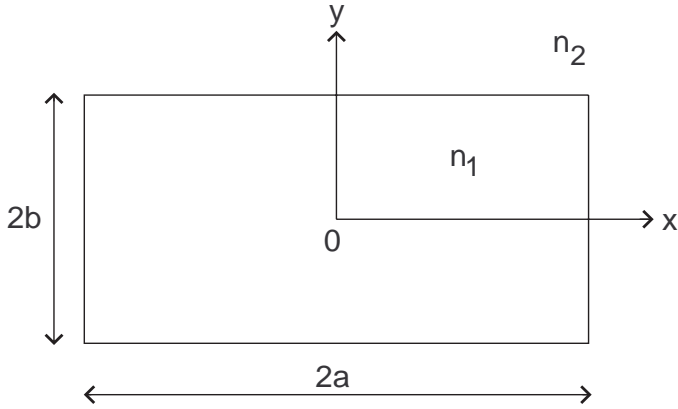
Fig. 2. Structure of a rectangular core optical waveguide.

refractive index profile of the optical waveguide under consideration. Moreover,

$$P_{j,i} = \rho^2(I_5 + I_6) \qquad (28)$$

correspond to polarization correction. The six integrals I_1 to I_6 is given in the Appendix as (29) to (34) and can be evaluated analytically in terms of sum of trigonometric functions if the refractive index profile $n(x,y)$ is approximated by rectangules of uniform refractive index.

The double summation series in (20) can be written as a matrix eigenvalue equation, $\mathbf{Ma} = W^2\mathbf{a}$, by defining a vector $\mathbf{a}$ consisting of the elements a_i and a matrix $\mathbf{M}$ composed of the coefficients $S_{j,i}$ and $P_{j,i}$. LAPACK subroutines are used to solve this equation [7], the propagation constants of the bound modes of a waveguide are calculated from the real, positive eigenvalues W^2 and the corresponding modal field is calculated via the Fourier coefficients of associated eigenvectors $\mathbf{a}$.

III. NUMERICAL RESULTS

A. Rectangular core optical waveguide

Figure 2 shows a optical waveguide with a rectangular core of width $2a$ and height $2b$. The core and cladding refractive index are $n_{co} = n_1 = 1.5$ and $n_{cl} = n_2 = 1.45$. $\lambda = 1.15\mu m$ and $a/b = 2$. Table I gives the normalized propagation constants $P^2 = [(\beta/k)^2 - n_{cl}^2]/(n_{co}^2 - n_{cl}^2)$ for the fundamental quasi-vector modes as a function of $2V_b/\pi$ where $V_b = kb(n_1^2 - n_2^2)^{1/2}$. The bound modes are denoted as E_{mn}^x mode for the quasi-TE mode and E_{mn}^y mode for the quasi-TM mode respectively. The m and n are both positive integers meaning $m-1$ and $n-1$ field zeros in the x and y directions of the modal fields respectively. The calculated results are in excellent agreement with Fourier operator transform (F-OPT) method [8] except at $2V_b/\pi$ equal 0.4 where present method is more accurate as shown by the convergence of P^2. The modal fields at $2V_b/\pi = 0.5$ is shown Fig. 3. As can be clearly seen the present method is able to reproduce the discontinuity in the field at the core-cladding boundaries, vertical side walls for quasi-TE mode and horizontal side walls for quasi-TM mode.

Results of P^2 for the first six bound modes of another rectangular core waveguide with high refractive index contrast, $n_1 = 2$, $n_2 = 1$, is shown in Table II. The associated field of these modes are shown in Fig. 4. Here, $V_b = 3$ and $a/b = 5/3$.

TABLE I

P^2 AS A FUNCTION OF $2V_b/\pi$ FOR THE FUNDAMENTAL QUASI-VECTOR MODES OF THE RECTANGULAR CORE OPTICAL WAVEGUIDE. $\alpha_x = a$, $\alpha_y = b$, $\rho = \sqrt{ab}$, AND $N_m^e = N_n^e = N$. THE PARAMETERS N_m^e AND N_n^e INDICATE THE NUMBER OF EVEN SPATIAL FREQUENCY COMPONENTS USED IN THE x AND y DIRECTIONS

| $2V_b/\pi$	N				F-OPT
	10	15	20	25	
E_{11}^x mode					
0.40	0.0346	0.0343	0.0337	0.0335	0.0400
0.45	0.0679	0.0664	0.0661	0.0661	0.0670
0.50	0.1077	0.1069	0.1069	0.1069	0.1068
0.55	0.1523	0.1522	0.1523	0.1522	0.1520
0.60	0.1991	0.1993	0.1992	0.1992	0.1990
0.65	0.2458	0.2459	0.2459	0.2458	0.2456
0.70	0.2909	0.2910	0.2910	0.2909	0.2907
0.75	0.3338	0.3339	0.3338	0.3338	0.3336
0.80	0.3741	0.3742	0.3741	0.3741	0.3739
0.85	0.4117	0.4118	0.4117	0.4117	0.4116
0.90	0.4467	0.4467	0.4467	0.4467	0.4465
0.95	0.4791	0.4791	0.4791	0.4791	0.4789
1.00	0.5090	0.5091	0.5091	0.5091	0.5089
E_{11}^y mode					
0.40	0.0274	0.0315	0.0320	0.0307	0.0483
0.45	0.0603	0.0617	0.0614	0.0614	0.0612
0.50	0.0999	0.1004	0.1000	0.1005	0.1003
0.55	0.1444	0.1443	0.1440	0.1444	0.1441
0.60	0.1908	0.1903	0.1901	0.1902	0.1900
0.65	0.2370	0.2363	0.2361	0.2361	0.2359
0.70	0.2817	0.2810	0.2809	0.2808	0.2805
0.75	0.3243	0.3237	0.3236	0.3235	0.3232
0.80	0.3645	0.3640	0.3639	0.3638	0.3635
0.85	0.4021	0.4018	0.4017	0.4016	0.4013
0.90	0.4372	0.4370	0.4369	0.4368	0.4365
0.95	0.4698	0.4697	0.4696	0.4695	0.4692
1.00	0.5001	0.5000	0.5000	0.4998	0.4996
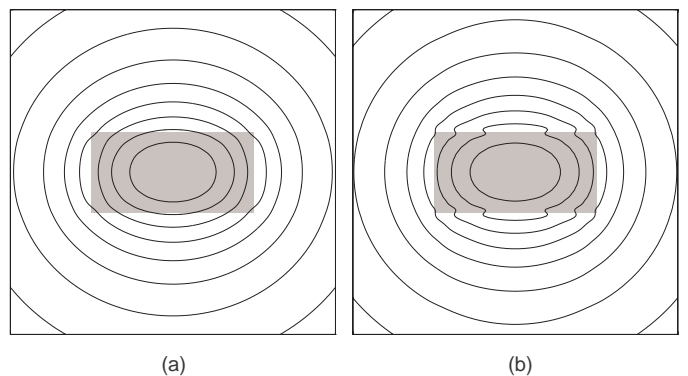
Fig. 3. Field pattern of (a) e_x of E_{11}^x mode and (b) e_y of E_{11}^y mode at $2V_b/\pi = 0.5$ for $N = 25$. The core region is shaded. Contour lines are at 10% intervals of peak amplitude.

TABLE II
P^2 OF THE FIRST SIX BOUND MODES OF THE HIGH REFRACTIVE INDEX
CONTRAST RECTANGULAR CORE WAVEGUIDE. $N_m^e = N_n^e = N$ FOR
MODES (a), (b) AND (f); $N_m^o = N_n^e = N$ FOR MODES (c) AND (d); AND
$N_m^e = N_n^o = N$ FOR MODE (e). THE PARAMETERS $N_m^{e,o}$ AND $N_n^{e,o}$
INDICATE THE NUMBER OF EVEN AND ODD SPATIAL FREQUENCY
COMPONENTS USED IN THE x AND y DIRECTIONS RESPECTIVELY

N	Mode					
	(a)	(b)	(c)	(d)	(e)	(f)
	E_{11}^x	E_{11}^y	E_{21}^y	E_{21}^x	E_{12}^x	E_{31}^y
10	0.7591	0.7007	0.5041	0.5000	0.3390	0.1979
15	0.7585	0.6968	0.5008	0.4991	0.3386	0.1961
20	0.7584	0.6972	0.5012	0.4961	0.3386	0.1965
25	0.7580	0.6953	0.4995	0.4962	0.3382	0.1950
30	0.7580	0.6960	0.5001	0.4947	0.3383	0.1955
H-G[4]	0.7577	0.6949	0.4988	0.4985	0.3375	0.1942

TABLE III
P^2 AS A FUNCTION OF FIBER PARAMETER $V = k\rho(n_1^2 - n_2^2)^{1/2}$ FOR THE
FUNDAMENTAL QUASI-VECTOR MODES OF THE CIRCULAR CORE OPTICAL
FIBER. $\alpha_x = \alpha_y = \rho$ AND $N_m^e = N_n^e = N$

V	Mode					
	E_{11}^x				E_{11}^y	HE_{11}
	N				N	
	10	15	20	25	=25	
0.8	—	0.0043	0.0049	0.0046	0.0047	0.0043
1.0	0.0339	0.0330	0.0325	0.0325	0.0325	0.0322
1.2	0.0920	0.0918	0.0918	0.0918	0.0918	0.0911
1.4	0.1696	0.1692	0.1691	0.1690	0.1689	0.1681
1.6	0.2510	0.2506	0.2505	0.2504	0.2503	0.2494
1.8	0.3286	0.3283	0.3281	0.3280	0.3280	0.3270
2.0	0.3991	0.3988	0.3987	0.3986	0.3985	0.3976
2.2	0.4615	0.4613	0.4612	0.4611	0.4610	0.4603
2.4	0.5163	0.5161	0.5160	0.5159	0.5158	0.5151
2.6	0.5640	0.5639	0.5638	0.5637	0.5636	0.5630
2.8	0.6056	0.6055	0.6054	0.6054	0.6053	0.6048
3.0	0.6420	0.6419	0.6418	0.6418	0.6417	0.6412

(a)　(b)　(c)　(d)　(e)　(f)

Fig. 4. (a)-(f) Field patterns, e_x for quasi-TE mode and e_y for quasi-TM mode, of the first six bound modes of the high contrast rectangular core waveguide for $N = 30$. Designation of the modes are given in Table II.

Results of P^2 are in good agreement with results using Hermite-Gauss (H-G) basis functions [4]. This is expected as present method with sine basis functions in the transformed domains have field zero at infinity as Hermite-Gauss basis functions does.

B. Step-index core optical fiber

The next structure to be studied is a circular core optical fiber (Fig. 5) with $n_{co} = n_1 = 1.6$ and $n_{cl} = n_2 = 1.5$. The first quadrant of the circular core is resembled by 25 unifrom rectangles and the rest is found by symmetry. P^2 of the two fundamental quasi-vector modes are almost the same as listed in Table III. Theoretically, with infinite number of rectangles, the fundamental quasi-vector modes are degenerated. Results of present quasi-vector solutions are compared with the exact vector solutions [6], HE_{11} mode, and they are in good agreement. The field patterns of the quasi-vector modes at $V = 1$ is
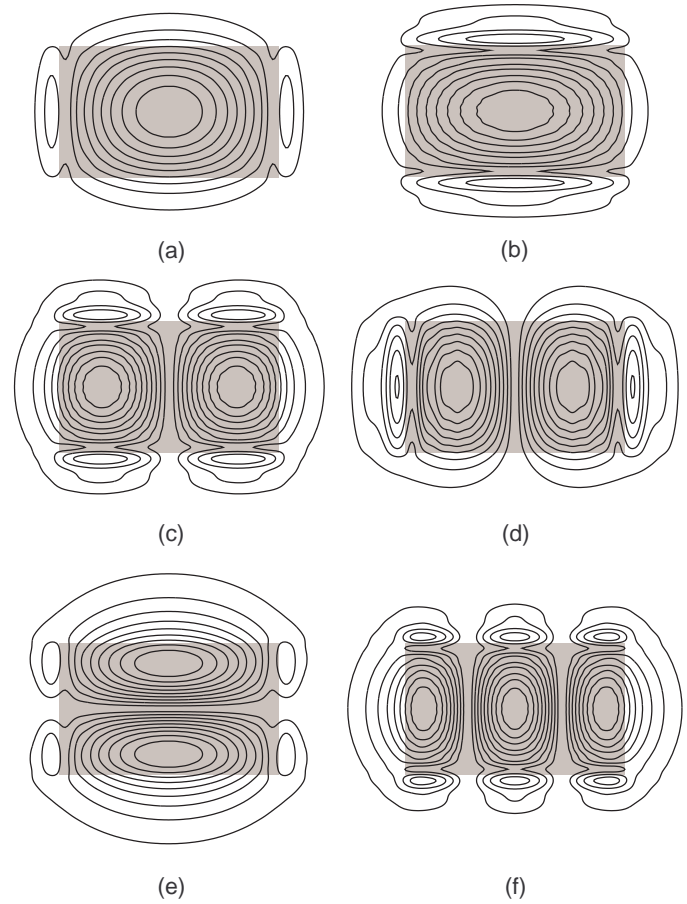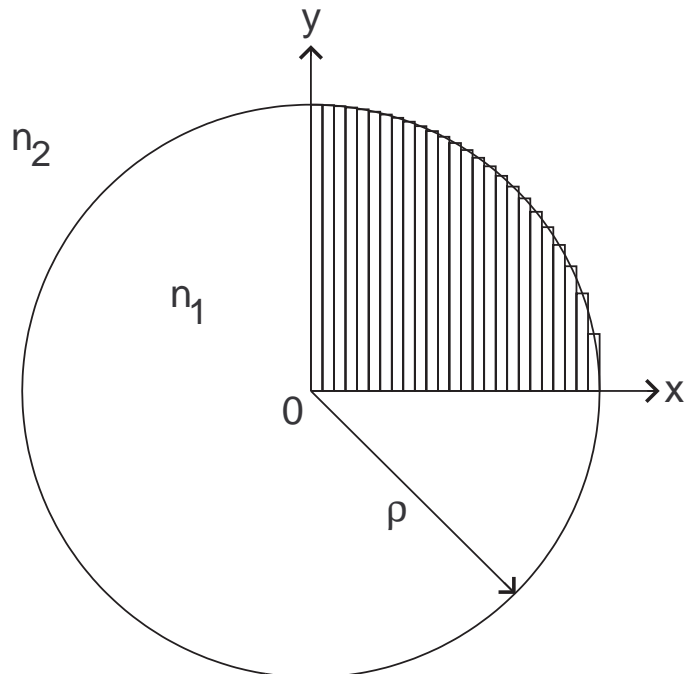

Fig. 5. Structure of a circular core optical fiber.
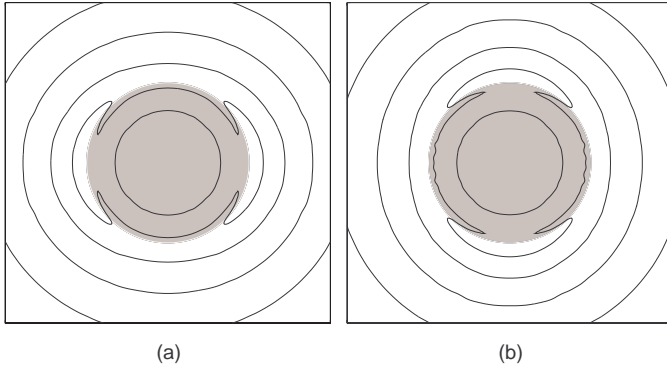
Fig. 6. Field patterns of (a) e_x of E_{11}^x mode and (b) e_y of E_{11}^y mode of the circular core optical fiber at $V = 1$ for $N = 25$.

given in Fig. 6. Discontinuity of field is clearly seen at the core-cladding boundary. The field component e_x of E_{11}^x mode along the x axis as a function of normalized distance $X = x/\rho$ is shown in Fig. 7(a). As can be seen from the figure, the quasi-vector modal fields are agree with the exact vector solution except near the core-cladding boundary which is detailed in Fig. 7(b). From this figure, e_x of quasi-TE mode near the boundary is likely to be an average of the exact vector solution and it is converge moderately to the exact vector solution as N is increased.

C. Rib optical waveguide

A rib optical waveguide as shown in Fig. 8 is considered in this section. Here, $n_{\mathrm{co}} = n_1 = 3.44$, $n_{\mathrm{cl}} = n_2 = 3.4$, $n_3 = 1$, $t = 1\mu m$, $w = 3\mu m$ and $\lambda = 1.15\mu m$. Table IV shows P^2 for the fundamental quasi-vector modes as a function of d. By comparison with results from F-OPT method [8] and beam propagation method (BPM) [9], the convergence of present solutions is better for E_{11}^x mode than E_{11}^y mode. This could be explained by the fact that higher spatial frequency components are needed to model the large discontinuity of field component e_y of E_{11}^y mode at the core-air interfaces perpendicular to y axis of Fig. 8 which are clearly seen form the field patterns at Fig. 9.

D. IID MQW waveguide

The last example is to apply present method to multiple quantum well (MQW) waveguide fabricated by impurity induced disordering (IID) technique [10]. The IID technique provides an efficient way to realize waveguiding structure in optoelectronic integrated circuits [11]. The structure to be modeled consists of $\mathrm{Al}_{0.3}\mathrm{Ga}_{0.7}\mathrm{As}/\mathrm{GaAs}$ QWs and thick $\mathrm{Al}_{0.3}\mathrm{Ga}_{0.7}\mathrm{As}$ buffer layer grown on a GaAs substrate; the schematic of the structure is shown in Fig. 10. In our model, Ga^+ ion is implanted with a projected range located around the center of the QW layers. The implantation process produces a modification of the QW material which in turn leads to differences in refractive index in different region [10]. The implanted region has a lower refractive index than the non-implanted region, hence produce lateral confinement of light. Figure 11 shows a IID MQW refractive index profile which is represented by rectangles of constant refractive index. The profile was calculated for $2a = 3\mu m$, $2b = 0.6\mu m$ at $\lambda = 0.901085\mu m$. The maximum and minimum refractive in-
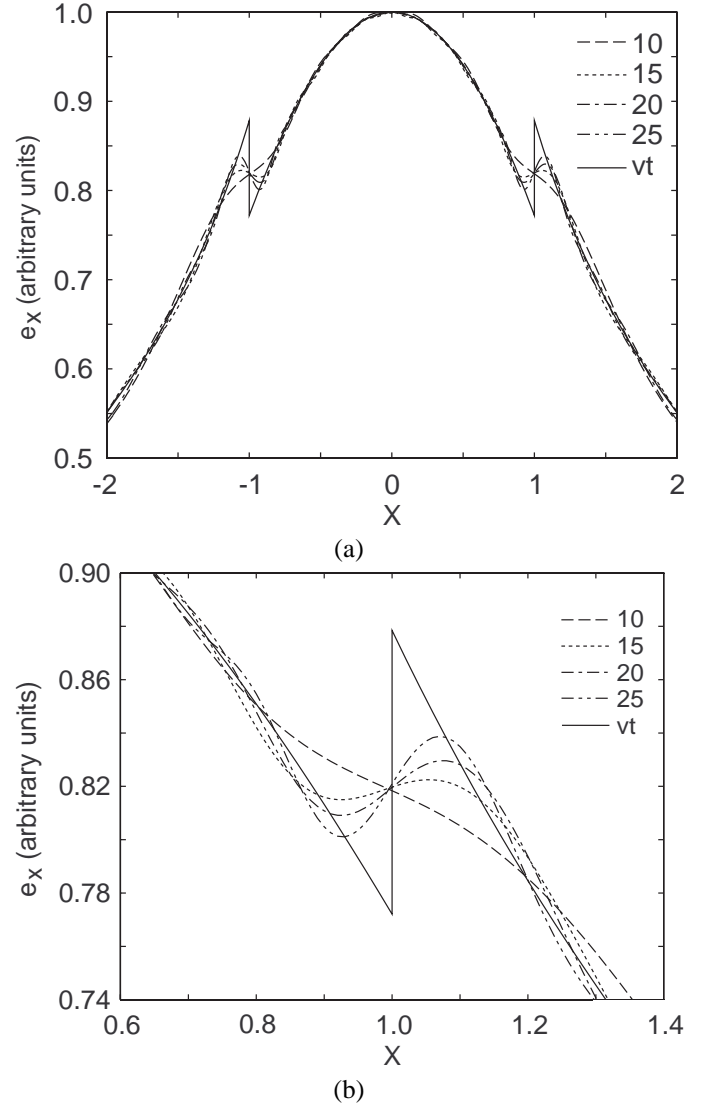

(a)

(b)

Fig. 7. (a) Electric field component e_x of quasi-TE mode as a function of normalized distance X for $N = 10, 15, 20$ and 25. The electric field component e_x of the exact vector (vt) solution is given in solid line. (b) Details of (a) near $X = 1$.
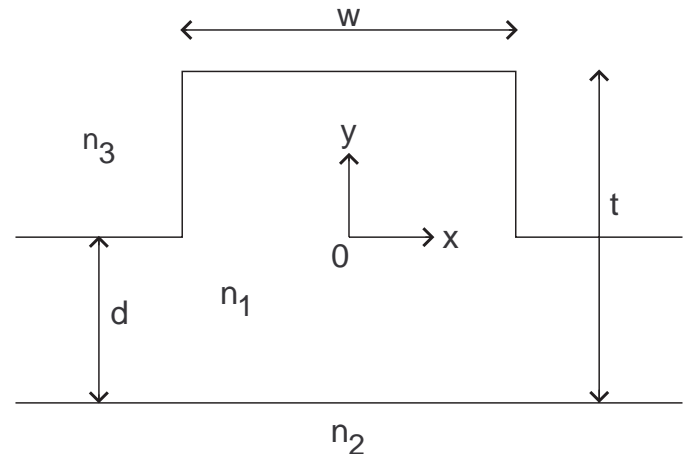

Fig. 8. Structure of a rib optical waveguide.

TABLE IV

P^2 AS A FUNCTION OF d FOR FUNDAMENTAL QUASI-VECTOR MODES OF THE RIB OPTICAL WAVEGUIDE. $\alpha_x = w/2$, $\alpha_y = t/2$, $\rho = \sqrt{\alpha_x \alpha_y}$, $N_m^e = N$ AND $N_n = 2N$

d	N			F-OPT	BPM
	10	20	30		
$\mathrm{E_{11}^x}$ mode					
0.0	0.2879	0.2961	0.2971	0.2992	0.3001
0.1	0.2911	0.2989	0.2997	0.3018	0.3026
0.2	0.2957	0.3029	0.3036	0.3055	0.3066
0.3	0.3019	0.3084	0.3091	0.3108	0.3116
0.4	0.3101	0.3158	0.3163	0.3178	0.3188
0.5	0.3202	0.3251	0.3255	0.3267	0.3269
0.6	0.3324	0.3364	0.3368	0.3373	0.3380
0.7	0.3468	0.3500	0.3503	0.3509	0.3504
0.8	0.3639	0.3666	0.3667	0.3668	0.3655
0.9	0.3859	0.3880	0.3886	0.3880	0.3871
1.0	0.4241	0.4268	0.4271	0.4273	0.4273
$\mathrm{E_{11}^y}$ mode					
0.0	0.2495	0.2559	0.2567	0.2652	0.2664
0.1	0.2523	0.2581	0.2588	0.2678	0.2685
0.2	0.2561	0.2614	0.2619	0.2703	0.2720
0.3	0.2615	0.2659	0.2664	0.2746	0.2762
0.4	0.2682	0.2719	0.2723	0.2804	0.2823
0.5	0.2769	0.2798	0.2800	0.2880	0.2892
0.6	0.2877	0.2896	0.2898	0.2976	0.2990
0.7	0.3002	0.3016	0.3017	0.3095	0.3101
0.8	0.3161	0.3166	0.3166	0.3244	0.3237
0.9	0.3367	0.3370	0.3367	0.3446	0.3441
1.0	0.3765	0.3769	0.3769	0.3851	0.3854

Fig. 10. Schematic of an IID MQW waveguide.
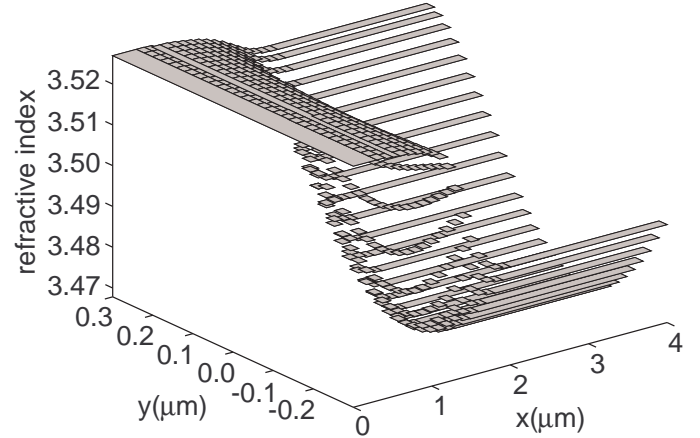
Fig. 11. Refractive index profile (half symmetry) of the IID MQW waveguide.

Fig. 9. Field patterns, e_x of $\mathrm{E_{11}^x}$ mode (left side) and e_y of $\mathrm{E_{11}^y}$ mode (right side), of the rib waveguide for $N = 30$ at (a)-(b) $d = 0\mu m$, (c)-(d) $d = 0.5\mu m$, and (e)-(f) $d = 1\mu m$.

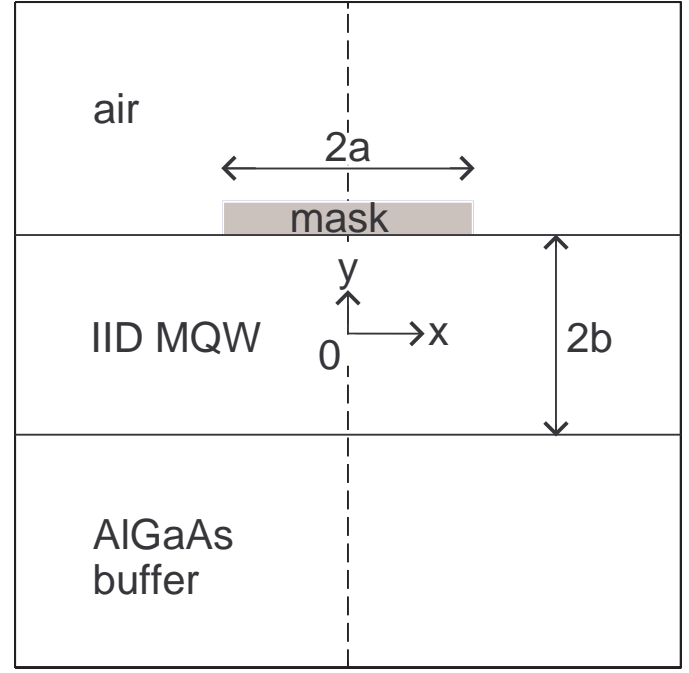dex are assigned as $n_{co}(= 3.52695)$ and $n_{cl}(= 3.46782)$ respectively. Other parameters are refractive index of $\mathrm{Al_{0.3}Ga_{0.7}As}$ buffer layer and air cover which is equal to 3.35447 and 1 respectively. P^2 of the fundamental quasi-vector modes are listed in Table V. The associated modal fields are shown in Fig. 12. Results show that present method is applicable for finding the waveguiding properties of an optical waveguide with a diffused refractive index profile.

IV. CONCLUSION

A numerical method for solving the guided quasi-vector modes problem of optical waveguide with aribtrary refractive index in a mapped infinite domains is described. Solving the problem with the Galerkin's method, the mode field is expanded into a two dimensional Fourier sine series and resulting in a matrix eigenvalue equation which is solved using the LAPACK subroutines.

TABLE V
P^2 FOR THE FUNDAMENTAL QUASI-VECTOR MODES OF THE IID MQW
WAVEGUIDE. $\alpha_x = a$, $\alpha_y = b$, AND $\rho = \sqrt{ab}$

N_m^e	N_n	Mode	
		E_{11}^{x}	E_{11}^{y}
10	20	0.1352	0.0110
15	30	0.1375	0.0111
20	40	0.1380	0.0096
25	50	0.1382	0.0094

(a)

(b)
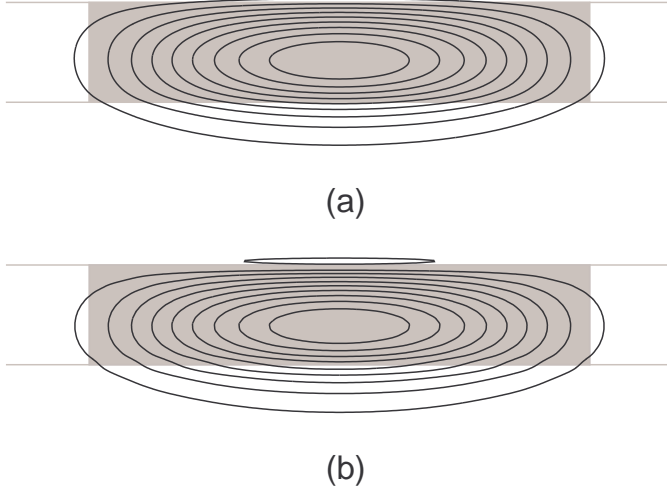
Fig. 12. Field patterns of (a) e_x of E_{11}^{x} mode and (b) e_y of E_{11}^{y} mode of the IID MQW waveguide for $N = 25$. The shaded region is the MQW under the mask.

The accuracy of present method is compared with the Fourier operator transform method and the beam propagation method for a rectangular core waveguide and a rib waveguide. Moreover, solutions for step-index circular core optical fiber are compared with the exact vector solution. Results shown that the present quasi-vector solutions provide a good approximation of the exact solution.

The application of present method to a waveguide with diffused refractive index profile is demonstrated using a multiple quantum well waveguide fabricated by impurity induced disordering technique. The normalized propagation constants of the fundamental quasi-vector modes converge moderately as we increase the number of spatial frequencies.

APPENDIX

The integrals I_1 to I_6 in (23) and (28) are given as follows:

$$
\begin{aligned}
I_1 &= -m_i^2 \pi^2 \int_{u=0}^{1} \int_{v=0}^{1} \left(\frac{du}{dx}\right)^2 \phi_i(u,v)\phi_j(u,v) du dv \\
&= -\frac{m_i^2}{2\alpha_x^2} \left\{ \frac{3\delta_{m_i,m_j}}{4} - \frac{\delta_{m_i,m_j-2}}{2} - \frac{\delta_{m_i,m_j+2}}{2} \right. \\
&\quad + \frac{\delta_{m_i,2-m_j}}{2} + \frac{\delta_{m_i,m_j-4}}{8} + \frac{\delta_{m_i,m_j+4}}{8} \\
&\quad \left. - \frac{\delta_{m_i,4-m_j}}{8} \right\} \delta_{n_i,n_j} ,
\end{aligned}
\tag{29}
$$

$$
\begin{aligned}
I_2 &= m_i \pi \int_{u=0}^{1} \int_{v=0}^{1} \left(\frac{d^2 u}{dx^2}\right) \frac{1}{\tan(m_i \pi u)} \\
&\quad \times \phi_i(u,v)\phi_j(u,v) du dv \\
&= \frac{m_i}{\alpha_x^2} \left\{ \frac{\delta_{m_i,2-m_j}}{4} + \frac{\delta_{m_i,m_j-2}}{4} - \frac{\delta_{m_i,m_j+2}}{4} \right. \\
&\quad \left. - \frac{\delta_{m_i,4-m_j}}{8} - \frac{\delta_{m_i,m_j-4}}{8} + \frac{\delta_{m_i,m_j+4}}{8} \right\} \delta_{n_i,n_j} ,
\end{aligned}
\tag{30}
$$

$$
\begin{aligned}
I_3 &= -n_i^2 \pi^2 \int_{u=0}^{1} \int_{v=0}^{1} \left(\frac{dv}{dy}\right)^2 \phi_i(u,v)\phi_j(u,v) du dv \\
&= -\frac{n_i^2}{2\alpha_y^2} \left\{ \frac{3\delta_{n_i,n_j}}{4} - \frac{\delta_{n_i,n_j-2}}{2} - \frac{\delta_{n_i,n_j+2}}{2} \right. \\
&\quad + \frac{\delta_{n_i,2-n_j}}{2} + \frac{\delta_{n_i,n_j-4}}{8} + \frac{\delta_{n_i,n_j+4}}{8} \\
&\quad \left. - \frac{\delta_{n_i,4-n_j}}{8} \right\} \delta_{m_i,m_j} ,
\end{aligned}
\tag{31}
$$

$$
\begin{aligned}
I_4 &= n_i \pi \int_{u=0}^{1} \int_{v=0}^{1} \left(\frac{d^2 v}{dy^2}\right) \frac{1}{\tan(n_i \pi v)} \\
&\quad \times \phi_i(u,v)\phi_j(u,v) du dv \\
&= \frac{n_i}{\alpha_y^2} \left\{ \frac{\delta_{n_i,2-n_j}}{4} + \frac{\delta_{n_i,n_j-2}}{4} - \frac{\delta_{n_i,n_j+2}}{4} \right. \\
&\quad \left. - \frac{\delta_{n_i,4-n_j}}{8} - \frac{\delta_{n_i,n_j-4}}{8} + \frac{\delta_{n_i,n_j+4}}{8} \right\} \delta_{m_i,m_j} ,
\end{aligned}
\tag{32}
$$

$$
\begin{aligned}
I_5 &= m_i \pi \int_{u=0}^{1} \int_{v=0}^{1} 2\left(\frac{du}{dx}\right)^2 \frac{1}{\tan(m_i \pi u)} \\
&\quad \times \phi_i(u,v)\phi_j(u,v) \frac{\partial \ln(n)}{\partial u} du dv \\
&\quad + \int_{u=0}^{1} \int_{v=0}^{1} 2\left(\frac{du}{dx}\right)^2 \phi_i(u,v)\phi_j(u,v) \\
&\quad \times \frac{\partial^2 \ln(n)}{\partial u^2} du dv \\
&= \frac{1}{\alpha_x^2} \int_{u=0}^{1} du \int_{v=0}^{1} dv \{\ln(n) \\
&\quad \times \{\{16[c(2u) - c(4u)] \\
&\quad - m_j^2[c(4u) - 4c(2u) + 3]s_i(u)s_j(u)s_i(v)s_j(v)\} \\
&\quad + m_i m_j[c(4u) - 4c(2u) + 3]c_i(u)c_j(u)s_i(v)s_j(v) \\
&\quad - 4m_i[s(4u) - 2s(2u)]c_i(u)s_j(u)s_i(v)s_j(v) \\
&\quad - 8m_j[s(4u) - 2s(2u)]s_i(u)c_j(u)s_i(v)s_j(v)\}\} ,
\end{aligned}
\tag{33}
$$

$$
\begin{aligned}
I_6 &= \int_{u=0}^{1} \int_{v=0}^{1} 2\left(\frac{d^2 u}{dx^2}\right) \phi_i(u,v)\phi_j(u,v) \frac{\partial \ln(n)}{\partial u} du dv \\
&= \frac{2}{\alpha_x^2} \int_{u=0}^{1} du \int_{v=0}^{1} dv \{\ln(n) \\
&\quad \times \{4[c(4u) - c(2u)]s_i(u)s_j(u)s_i(v)s_j(v) \\
&\quad + m_i[s(4u) - 2s(2u)]c_i(u)s_j(u)s_i(v)s_j(v) \\
&\quad + m_j[s(4u) - 2s(2u)]s_i(u)c_j(u)s_i(v)s_j(v)\}\} .
\end{aligned}
\tag{34}
$$

In (33) and (34), sine related functions $s(2u) = \sin(2u)$, $s_i(u) = \sin(m_i \pi u)$, $s_i(v) = \sin(n_i \pi v)$, etc. For cosine related functions, they are abbreviated by the symbol c.

REFERENCES

[1] C. H. Henry and B. H. Verbeek, "Solution of the scalar wave equation for arbitrarily shaped dielectric waveguides by two-dimensional Fourier analysis," *J. Lightwave Technol.*, vol. 7, pp. 308–313, 1989.

[2] D. Marcuse, "Solution of the vector wave equation for general dielectric waveguides by the Galerkin method," *IEEE J. Quantum Electron.*, vol. 28, pp. 459–465, 1992.

[3] S. J. Hewlett and F. Ladouceur, "Fourier decomposition method applied to mapped infinite domains: Scalar analysis of dielectric waveguides down to modal cutoff," *J. Lightwave Technol.*, vol. 13, pp. 375–383, 1995.

[4] A. Weisshaar, J. Li, R. L. Gallawa, and I. C. Goyal, "Vector and quasi-vector solutions for optical waveguide modes using efficient Galerkin's method with Hermite-Gauss basis functions," *J. Lightwave Technol.*, vol. 13, pp. 1795–1800, 1995.

[5] K. S. Chiang, "Review of numerical and approximate methods for the modal analysis of general optical dielectric waveguides," *Opt. Quantum Electron.*, vol. 26, pp. S113–S134, 1994.

[6] A. W. Snyder and J. D. Love, *Optical Waveguide Theory*, Chapman and Hall, London, 1983.

[7] E. Anderson, Z. Bai, C. Bischof, J. Demmel, J. Dongarra, J. Du Croz, A. Greenbaum, S. Hammarling, A. McKenney, S. Ostrouchov, and D. Sorensen, *LAPACK Users's Guide*, S.I.A.M., Philadelphia, 2nd. edition, 1995.

[8] G. M. Berry, S. V. Burke, C. J. Smartt, T. M. Benson, and P. C. Kendall, "Exact and variational Fourier transform methods for analysis of multilayered planar waveguides," *IEE Proc. J.*, vol. 142, pp. 66–75, 1995.

[9] W. P. Huang and C. L. Xu, "Simulation of three-dimensional optical waveguides by a full-vector beam propagation method," *IEEE J. Quantum Electron.*, vol. 29, pp. 2639–2649, 1993.

[10] T. Wolf, C. L. Shieh, R. Engelmann, K. Alavi, and J. Mantz, "Lateral refractive index step in GaAs/AlGaAs multiple quantum well waveguides fabricated by impurity-induced disordering," *Appl. Phys. Lett.*, vol. 55, pp. 1412–1414, 1989.

[11] B. L. Weiss, "Quantum well mixing for optoelectronics," *Opt. Quantum Electron.*, vol. 23, pp. S799–S994, 1991.